Sand motion induced by oscillatory flows: sheet flow and vortex ripples

Jan S. Ribberink[1], Jebbe J. van der Werf[1] and Tom O'Donoghue[2]

[1] University of Twente, Faculty of Engineering, Water Engineering and Manage-ment, PO Box 217, 7500 AE Enschede, The Netherlands
j.s.ribberink@utwente.nl
[2] University of Aberdeen, Department of Engineering, King's College, Aberdeen AB24 3UE, Scotland

1 Introduction

Shoaling short gravity waves at sea approaching the shore become asymmetric and are able to generate a net resulting sand transport in cross-shore direction (on-shore-offshore transport). The wave-related sand transport is still very difficult to predict due to the complexity of its underlying processes, which mainly take place in a thin layer near the sea bed in the wave boundary layer (thickness of order centimeters). The development of models for cross-shore sand transport heavily relies on experimental lab research, especially as taking place in large oscillating water tunnels (see, e.g., Nielsen, 1992). In oscillating water tunnels the near-bed horizontal orbital velocity, as induced by short gravity waves, can be simulated above fixed or mobile sandy beds (for a detailed description, see, e.g., Ribberink and Al-Salem, 1994). It should be realized that the vertical orbital flow and relatively small wave-induced residual flows as streaming and drift are not reproduced in flow tunnels. Research aimed at their contribution to the net sediment motion under surface waves is still ongoing (see Ribberink et al., 2000).

The present study is focused at the sediment motion as occurring under the influence of horizontal oscillatory flows and measuring results will be presented of the Large Oscillating Water Tunnel (LOWT) of WL—Delft Hydraulics and the Aberdeen Oscillating Flow Tunnel (AOFT). Due to their large size (length of test sections: 10-15 m) they belong to the few available facilities in which the near-bed flows of full-scale waves can be generated and scale effects can be avoided.

Based on an energetics-approach Bagnold and Bailard (see Bailard, 1981) developed sand transport formulas for short gravity waves, relating the time-dependent sand transport rate during a wave-cycle $q_s(t)$ in a quasi-steady way to a power n of the horizontal velocity above the wave boundary layer $U(t)$:

Bernard J. Geurts et al. (eds), Particle Laden Flow: From Geophysical to Kolmogorov Scales, 3–14.

$$q_s(t) = m|U(t)|^{n-1}U(t) \tag{1}$$

Ribberink (1998) developed a similar quasi-steady formula based on the time-dependent bed-shear stress. For asymmetric waves this type of transport-formulas always leads to a time-averaged (net) transport rate which is 'on-shore' directed.

All net transport rate measurements which were collected during the preceding years in the LOWT and the AOFT for asymmetric waves are depicted in Figure 1 as a function of the sediment mobility number $\Psi = 2U_{rms}^2/\Delta g D$ (with U_{rms} the root mean square velocity of the wave, Δ the relative density of sand, D the grain diameter and g the gravitational acceleration).

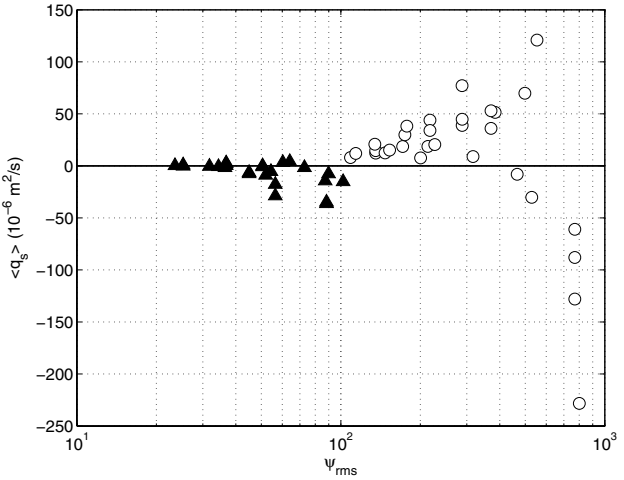

Fig. 1. Measured net sand transport rates $\langle q_s \rangle$ under asymmetric oscillatory flows as a function of the mobility number Ψ in the vortex ripple regime (triangles) and the sheet flow regime (circles). The data refer to flows with a constant degree of asymmetry $R = U_c/(U_c + U_t) = 0.62$, wave periods $T = 3 - 9$ s and sand with grain diameters $D = 0.13 - 0.45$ mm.

It is shown that - contrary to what transport model (1) suggests - the net transport rates can be 'on-shore' (> 0) as well as 'offshore' directed (< 0). Moreover, two data groups with different micro bed morphology can be observed : i) a vortex ripple regime ($\Psi < 100 - 200$) with mainly 'offshore' transport, and ii) a sheet flow regime with flat sea beds ($\Psi > 100 - 200$) with mainly 'on-shore' transport.

In order to obtain a better understanding of this variable behavior of the net sand transport, in the present paper the underlying boundary layer flow and sediment dynamics of these two bed regimes are discussed. Here-to insights as obtained during a series of Ph.D. studies in the preceding years (Dohmen-Janssen, 1999; Clubb, 2001; Wright, 2002; Hassan, 2003; Van der

Werf, 2006) are presented and different types of sand transport models are reviewed.

2 Oscillatory sheet flow

For large mobility numbers ($\Psi > 100 - 200$) ripples are washed out and the sea bed becomes plane. The oscillatory sand transport is now confined to a thin layer with a thickness of order $1cm$ near the bed, in which large sediment concentrations (10-50 volume percent) and large sand fluxes can occur (sheet flow layer).

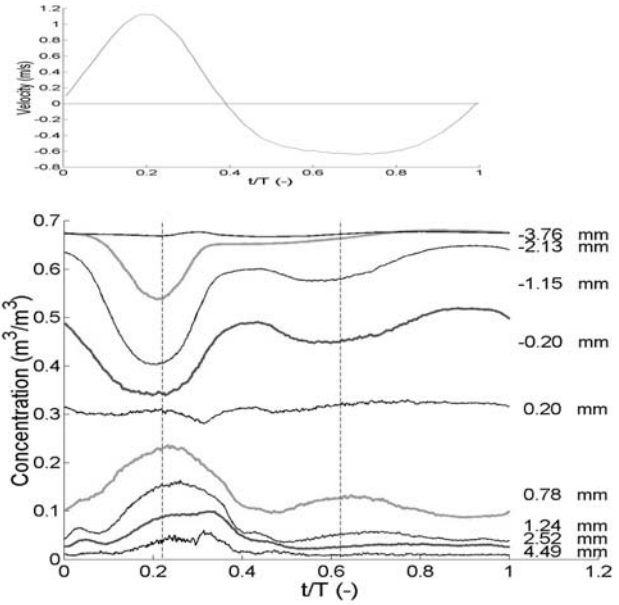

Fig. 2. Time-dependent flow velocity in the free stream (upper panel) and sand (volume) concentrations at different elevations in the sheet flow layer during 1 asymmetric wave cycle (experiment Mh, 0.2 mm sand).

Ribberink and Al-Salem (1995) and McLean et al. (2001) showed how small Conduction Concentration probes (CCM) can be used to visualize and measure the sand pick-up and redeposition processes in the sheet flow layer. The probes measure sand concentration and grain-velocity through electro-resistance of the sand water mixture (sensing volume of ca. 1 mm high).

Asymmetric gravity waves on the shore-face induce a horizontal oscillatory flow with a relatively large maximum velocity in on-shore direction velocity U_c (under the wave crest) and a relatively small maximum velocity in off-shore direction U_t (under the wave trough). Figure 2 shows time-dependent

ensemble-averaged sand concentrations during an asymmetric wave cycle, as measured with CCM, at different elevations in the sheet flow layer ($z = 0\ mm$ refers to the original bed level without sand motion). The upper panel shows the horizontal asymmetric velocity in the free stream (above the wave boundary layer). The data were measured with 0.2 mm sand and reveal a two-layer structure of the near-bed sand transport layer, with a pick-up layer ($z < 0$) and an upper sheet flow layer ($z > 0$). During flow acceleration sand is picked up from the pick-up layer (decreasing concentrations) into the upper sheet flow layer (increasing concentrations). During flow deceleration the opposite occurs and sand settles back from the upper sheet flow layer into the pick-up layer. The upper elevations ($z = 0.78 - 4.49\ mm$) show an increasing phase-lag of the maximum concentration with increasing elevation. These phase-lag effects play a crucial role in the magnitude and direction of the mean resulting horizontal transport of asymmetric waves in the sheet flow regime (Dohmen-Janssen et al, 2002; Hassan, 2003).

Phase-lags may occur in the pick-up process of sand grains, in the vertical upward transport of sand and in the resettling process. Figure 3 shows how the concentrations, measured at a fixed level in the upper sheet flow layer and scaled with the time-averaged concentration C_m, experience increasing phase-lags for decreasing wave periods T.

Further systematic experiments revealed that the phase-lags also increase for decreasing grain size D (slower resettling) and for increasing free stream velocities (entrainment to higher elevations).

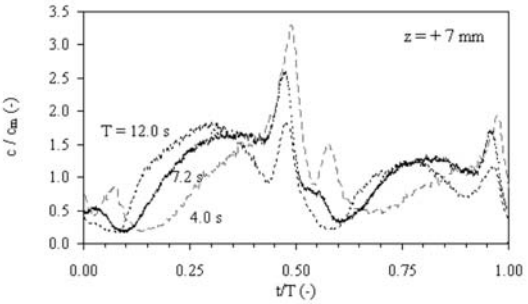

Fig. 3. Time-dependent volume concentrations at a fixed level $z = 7\ mm$ in the upper sheet flow layer during one wave cycle for three wave periods T. The concentrations are normalized with their mean values C_m.

Recently, O'Donoghue and Wright (2004) obtained further insight into the phase-lag phenomenon with high-resolution sand flux measurements using various sand sizes under asymmetric waves in the AOFT. They showed that for very fine sand (0.15 mm) the direction of the mean (horizontal) sand transport may even change sign (from 'on-shore' to 'offshore'), due to the fact that the (large) sand volumes stirred up during the (strong) 'on-shore'

half wave cycle, are still suspended in the wave boundary layer during the 'offshore' half cycle. As an illustration Figure 4 shows the measured horizontal maximum 'on-shore', maximum 'offshore' and total mean flux profiles for two grain sizes, i.e., 0.28 (MA5010) and 0.15 mm (FA5010).

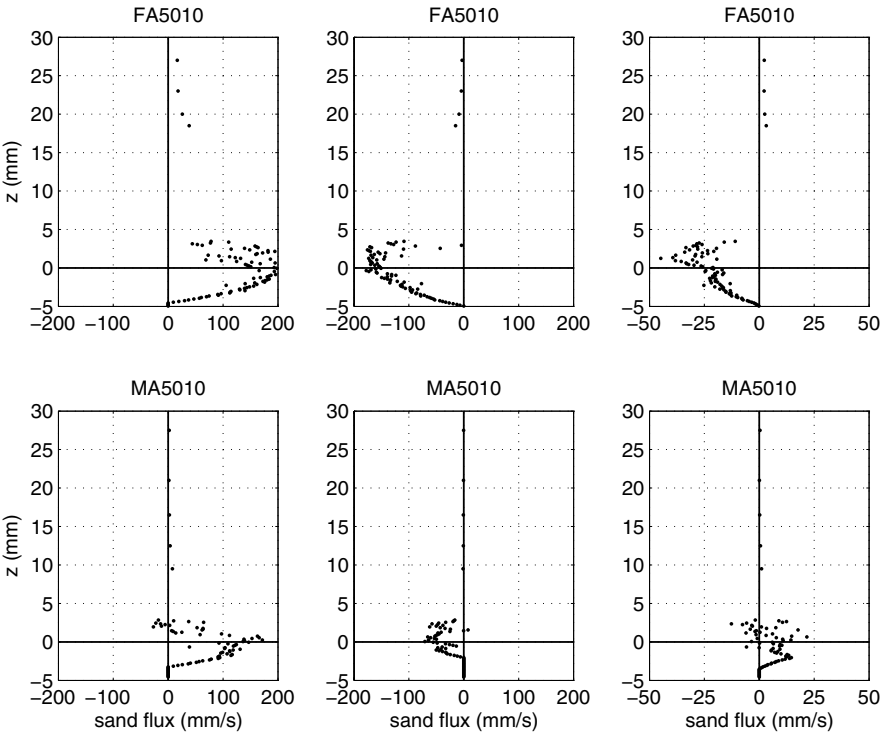

Fig. 4. Vertical profiles of horizontal sand flux for fine sand (0.15 mm; upper panels) and medium sand (0.28 mm; lower panels). Maximum 'on-shore' flux (left panels), maximum 'offshore' flux (middle panels) and time-averaged net flux (right panels).

Sand motion around oscillatory vortex ripples

Vortex ripples appear on the sea bed for mobility numbers $\Psi < 100 - 200$. Their dimensions, such as ripple height η (of the order $cm - dm$) and length λ (of the order $dm - m$), directly scale with the amplitude of the horizontal oscillatory motion near the sea bed, and show a variation with the mobility number (see Nielsen, 1992; O'Donoghue et al., 2006).

For an overview of present knowledge about this sand transport regime, reference is made to Van der Werf (2006). The flow dynamics in the vortex ripple regime differ strongly from the oscillatory sheet flow regime, mainly

due to the fact that processes as flow separation and coherent vortex motions now dominate the entrainment, transport and resettling of sand grains. The turbulence associated with this vortex shedding process leads to much thicker wave boundary layers and to a more important role of suspended sediment in the sand transport process than in sheet flow conditions.

Recently, new flow velocity and sand concentration measurements were carried out around natural mobile ripples under full-scale asymmetric waves in the AOFT (see Van der Werf, 2006). Advanced measuring instrumentation such as a.o. Particle Image Velocimetry (PIV) and an Acoustic Backscatter System (ABS) were used. Figure 5 shows an example of (grain) velocity vector fields at different moments during the wave cycle, as obtained with PIV.

The data reveal the development of a strong vortex at the lee side of the ripple during the first 'on-shore' directed half wave cycle, when the highest velocities occur (phases A,B,C,D). After flow reversal this vortex is transported over the ripple crest 'offshore' (phases E and F). During this half wave cycle the velocities are lower due to wave asymmetry, and a similar but less strong vortex develops at the other side of the ripple crest (phases G and H). After the next flow reversal this vortex is again transported over the ripple crest but now in 'on-shore' direction (phases A and B). This process of oscillatory vortex shedding leads to a boundary layer dominated by coherent vortex motions extending up to 2 ripple heights above the ripple crest.

Figure 6 shows the sand concentrations around the ripple, as measured with ABS during the same experiment, at three moments after flow reversal from 'on-shore' to 'offshore' ($t/T = 0.5, 0.56$ and 0.61, see upper plot of Figure 5). Sand - as trapped earlier during the 'on-shore' half wave cycle in the large lee-side vortex - is transported over the ripple crest directly after the flow reversed to the 'offshore' direction (to the left in Figure 6). Contrary to the sheet flow regime, most of the suspended sand is now transported with a considerable phase-lag of the order of 900 with respect to the free-stream velocity.

This specific 'offshore' flux of suspended sand often controls the total net transport as induced by the full asymmetric wave in the vortex ripple regime. If suspension is dominantly present, also the total net transport is generally 'off-shore' directed (< 0), because - due to the wave asymmetry - the strong ÔoffshoreÕ flux it is much stronger than its 'on-shore' counterpart.

3 1DV RANS modeling

Reynolds-averaged 1DV Navier-Stokes equations with different turbulence closures are combined with an advection-diffusion equation for suspended sediment concentrations and solved numerically to simulate time-dependent suspended sediment fluxes and sand transport by waves in flat sea bed conditions with sheet flow (see Ribberink and Al-Salem, 1995; Uittenbogaard and Klopman, 2001; Malarkey et al., 2003). In general the flow is driven by the

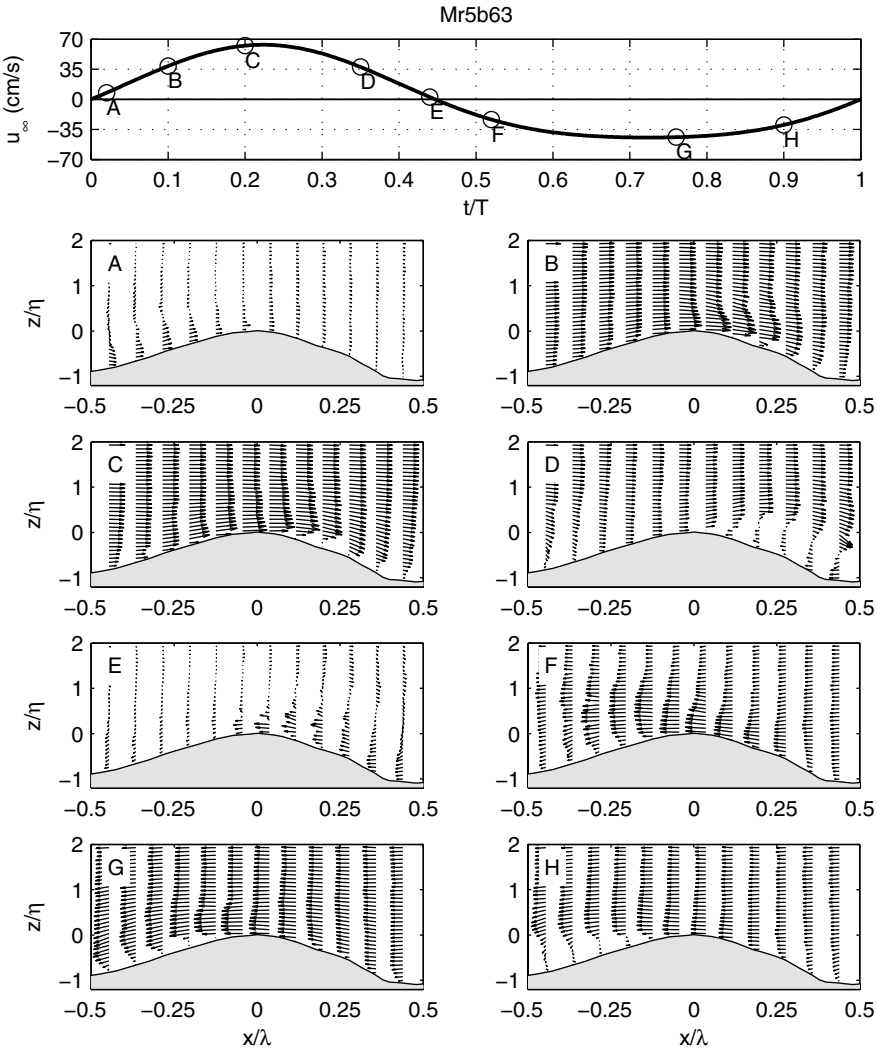

Fig. 5. Grain-velocity vector fields around a ripple at 8 phases during the wave cycle as measured with PIV (exp. Mr5b63) Positive, 'on-shore' flow is to the right. The top panel shows the free-stream orbital velocity u_∞ during the wave cycle. Vertical coordinate z and horizontal coordinate x are normalized with the ripple height η and respectively the ripple length λ.

time-dependent pressure-gradient near the sea bed and a rough wall boundary condition is assumed at the (fixed) bed level. A reference concentration at a level close to the bed is prescribed as a function of the time-dependent bed shear stress. The Point Sand Model (PSM) of Uittenbogaard and Klopman

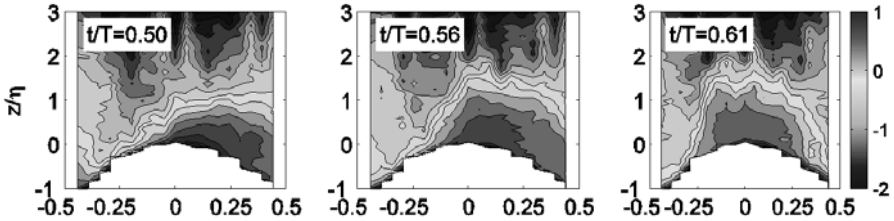

Fig. 6. Time-dependent concentration field around the ripple, as measured with ABS at 3 moments directly after flow reversal from 'on-shore' to 'offshore', i.e., $t/T = 0.5, 0.56$ and 0.61 (experiment Mr5b63), and showing the transport of the vortex filled with sand over the ripple crest.

(2001) is not confined to oscillatory flows but also includes wave-current interaction over the full water column. In PSM the equation for turbulent kinetic energy is provided with a buoyancy term, leading to turbulence suppression due to vertical concentration gradients (stratification). Moreover, a settling velocity reduction function is included, accounting for the hindered settling effect in case of large sediment concentrations.

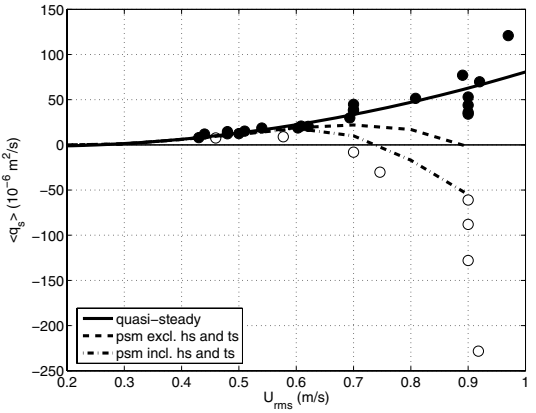

Fig. 7. Measured net transport rates (symbols) and predicted net transport rates with PSM (lines) for asymmetric waves as a function of U_{rms} (sheet flow regime). The solid line and black symbols refer to 3 medium sands (0.21, 0.32, 0.46 mm), the dashed lines and open symbols refer to 2 fine sands (0.13, 0.15 mm).

PSM is used to explain the phase-lag effects, occurring in oscillatory sheet flows, as discussed above. Figure 7 summarizes the results of this investigation by showing predicted and measured net transport rates as a function of U_{rms} (= root-mean-square velocity of the oscillatory flow velocity) for two fine sands

with $D_{50} = 0.13$ and $0.15\ mm$ and three medium sands with $D_{50} = 0.21,\ 0.32$ and $0.46\ mm$.

The measured transport rates are all from oscillatory flow experiments (LOWT and AOFT) with a small range in wave asymmetry ($R \approx 0.60 - 0.65$) and wave periods ($T = 5 - 9\ s$). In accordance with the data, PSM shows a distinct separation between positive ('on-shore') and negative ('offshore') transport rates for medium respectively fine sands. The medium sands behave in a quasi-steady way, showing increasing positive transport rates with increasing U_{rms} ($\langle q_s \rangle \sim U_{rms}^3$). The fine sands experience a substantial phase-lag effect, which is simulated by PSM ($D_{50} = 0.13\ mm$, $R = 0.62$, $T = 6.5\ s$) in a reasonable way. Inclusion of turbulence suppression and hindered settling effects in PSM leads to increased phase-lags and a better agreement between the data and the simulations. Nevertheless, it appears that the phase-lag effects as well as the negative transport rates are still underestimated by the model.

Similar conclusions follow from simulations with a two-layer model, provided with an empirical sheet flow layer description (Malarkey et al., 2003), and a two-phase flow model (see O'Donoghue et al., 2004). It is concluded that a better description of the time-dependent sand exchange between sea bed and sheet flow layer (pick-up and re-settling) is probably needed for further quantitative improvement of the models.

Using the new experimental tunnel data in the vortex ripple regime Van der Werf (2006) shows that - although this regime would require in principle a 2DV or 3D modeling approach - also a 1DV model with adjusted descriptions for eddy-viscosity and sediment entrainment is able to give a good description of the over-all time-dependent sand fluxes and net transport rates.

4 Unsteady sand transport formulas

The process-research as described above has stipulated the dominant role of phase-lag effects in the sand transport process by waves and their different character in the vortex ripple and sheet flow regime.

For the sheet flow regime the 'quasi-steady' transport model of Ribberink (1998) has therefore been adjusted to an 'unsteady' transport model. Hereto, the sheet flow concentrations are modeled in a schematic way as an advection-diffusion process with a constant eddy-viscosity ε_s and a simplified reference boundary condition. The equations are solved analytically for asymmetric oscillatory flows and a dimensionless phase-lag parameter is obtained, representing the ratio of sediment entrainment height above the bed (= sheet flow layer thickness) and the vertical settling distance of sediment during a wave period ($W_s T$). The sheet flow layer thickness δ_s is modeled as a function of the Shields parameter. Using this phase-lag model an unsteady transport formula is developed, which provides a strongly improved description of measured net

transport rates in the sheet flow regime. For more details see Dohmen-Janssen, et al. (2002) and Hassan (2003).

In the vortex ripple-regime the phase-lag effects are generated in a different way than in sheet flow conditions, due to the vortex shedding process. Apart from the strength of the lee-side vortices and the moment of their upward injection during the wave cycle (near flow reversal), also the potential of the sediments to be entrained into suspension in the lee-side vortex plays an important role.

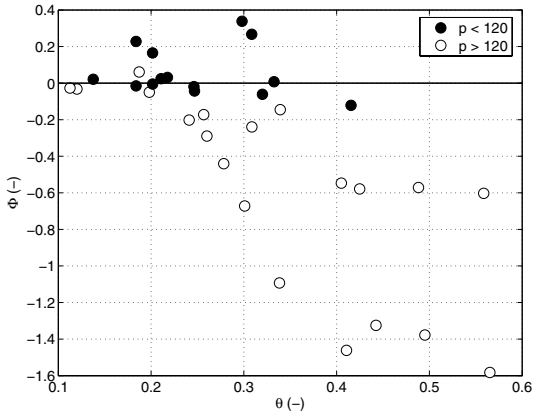

Fig. 8. Measured non-dimensional net transport rates Φ for asymmetric oscillatory flows in the vortex ripple regime as a function of the Shields parameter θ for 2 ranges of the vortex suspension parameter p. Positive Φ-values refer to 'on-shore' transport. The data are from oscillatory flow experiments with the same degree of asymmetry ($R = 0.6 - 0.63$), wave periods $T = 3 - 12$ s and grain-size $D_{50} = 0.21 - 0.44$ mm.

Figure 8 shows how - during asymmetric wave experiments (in AOFT and LOWT) - the direction and magnitude of the dimensionless mean transport rate Φ ($= \langle q_s \rangle / \sqrt{\Delta g D^3}$) is influenced by two parameters, i.e., the Shields parameter θ ($= f_w U_{rms}^2 / (\Delta g D)$) and a new vortex-suspension parameter $p = \eta / D$. The latter parameter, representing the ratio of the ripple height η (dimension of the vortex) and the grain-size D, indicates to what extent suspended sediment and associated phase-lag processes are important. For small p-values (small vortex/ coarse sediment) bed-load transport dominates and the net transport rates are mainly 'on-shore'. For large p-values (large vortex / fine sediment) suspended sediment is dominant and phase-lag effects lead to 'offshore' directed transport rates. The transport rates also tend to become more negative ('offshore' directed) for increasing Shields parameter. Using the available dataset of tunnel measurements in the vortex ripple regime, Van der Werf (2006) developed a new empirical unsteady sand transport formula, in which the vortex suspension parameter p is one of the key parameters.

5 Conclusions

An overview is given of experimental research in oscillating water tunnels (LOWT and AOFT) aimed at a better understanding of sand motion in oscillatory flows. Two different transport regimes were investigated using advanced measuring techniques (CCM, UVP, PIV, ABS), i.e., the vortex ripple regime and the sheet flow regime. New insights and detailed data were obtained of the unsteady flow processes controlling the total net sand transport under asymmetric waves. Phase-lag effects or time-history effects during the wave cycle strongly control whether net sand transport under asymmetric oscillatory flows is 'on-shore' or 'offshore' directed. The time-history effects in the two transport regimes show large differences, mainly due to the large differences in sand entrainment and transport mechanisms. In the vortex ripple regime vortex shedding and suspended sediment generally lead to large phase-lags and 'offshore' directed transport. Oscillatory sheet flow is often a more quasi-steady process with 'on-shore' directed sand transport, except for fine sand and short wave periods when phase-lag effects may lead to 'offshore' transport. It was shown that a RANS model, which includes hindered settling and turbulence suppression is able to explain the direction change from 'on-shore' to 'offshore' transport in the sheet flow regime in a qualitative sense. Based on the new insights new unsteady sand transport formulas were developed for the two bed-form regimes.

References

[1] Bailard, J.A. (1981): An energetics total load sediment transport model for a plane sloping beach. J. Geoph. Research, Vol. 86, No. C11, pp. 10938-10954.

[2] Clubb, G.S. (2001): Experimental study of vortex ripples in full-scale sinusoidal and asymmetric flows, PhD thesis, University of Aberdeen, Scotland.

[3] Dohmen-Janssen (1999): Grain size influence on sediment transport in oscillatory sheet flow, phase lags and mobile-bed effects. Ph.D. Thesis, Delft Univ. of Technology, The Netherlands.

[4] Dohmen-Janssen, C.M., D.F. Kroekenstoel, W.N.M. Hassan, and J.S. Ribberink (2002): Phase lags in oscillatory sheet flow: experiments and bed load modelling. J. Coast. Eng., Vol. 46, pp. 61-87.

[5] Hassan, W.N.M.H. (2003): Transport of size-graded and uniform sediments under oscilla-tory sheet-flow conditions, Ph.D. Thesis, University of Twente, The Netherlands

[6] Malarkey, J., A.G. Davies, Z.Li (2003): A simple model of unsteady sheet flow sediment transport, Coastal Eng. Vol. 48, pp 171-188.

[7] McLean, S.R., J.S. Ribberink, C.M. Dohmen-Janssen and W.N.M. Hassan (2001): Sediment transport measurements within the sheet flow layer

under waves and currents. J. Waterway, Port, Coast. and Ocean Eng., ISSN 0733-950X.

[8] Nielsen, P. (1992): Coastal bottom boundary layers and sediment transport, World Scien-tific, Singapore, 324 p.

[9] O'Donoghue, T. and Wright, S. (2004) : Flow tunnel measurements of velocities and fluxes in oscillatory sheet flow for well-sorted and graded sands, Coastal Eng. Vol. 51, pp 1163-1184

[10] O'Donoghue, T., Ming Li, J. Malarkey, S. Pan, A.G. Davies, B.A. O'Connor (2004): Numerical and experimental study of wave generated sheet flow, Proc. 29th Int. Conf. On Coast. Eng., Lisbon, Portugal , pp. 1690-1702.

[11] O'Donoghue, T., Doucette, J.S., Van der Wef J.J. and J.S.Ribberink (2006): The dimensions of sand ripples in full-scale oscillatory flows, accepted for publication in Coastal Engineering.

[12] Ribberink, J.S. and A.A. Al-Salem (1994): Sediment transport in oscillatory boundary layers in cases of rippled beds and sheet flow. J. Geophysical Research, Vol. 99, No. C6, pp. 12,707-12,727.

[13] Ribberink, J.S. and A.A. Al-Salem (1995): Sheet flow and suspension in oscillatory boundary layers. Coast. Eng., Vol. 25, pp. 205-225.

[14] Ribberink, J.S. (1998): Bed-load transport for steady flows and unsteady oscillatory flows. Coast. Eng., Vol. 34, pp. 59-82.

[15] Ribberink, J.S., Dohmen-Janssen, C.M., Hanes, D.M., McLean, S.R. and C. Vincent (2000): Near-bed sand transport mechanisms under waves - a large-scale flume experiment (Sistex99), In Proc. 27th Int. Conf. On Coast. Eng., Sydney, Australia, pp. 3263-3276.

[16] Uittenbogaard, R.E. (2000): 1DV Simulation of Wave Current Interaction. In Proc. 27th Int. Conf. On Coast. Eng., Sydney, Australia, pp. 255-268.

[17] Uittenbogaard, R.E. and G. Klopman (2001): Numerical simulation of wave-current driven sediment transport, Proc. Coastal Dynamics'01, ASCE, Lund, pp 568-577.

[18] Van der Werf, J.J. (2006): Sand transport over rippled beds in oscillatory flow, Ph.D. Thesis, University of Twente, The Netherlands

[19] Wright, S. (2002): Well-sorted and graded sands in oscillatory sheet flow, PhD thesis, Uni-versity of Aberdeen, Scotland.